

Long-term climatology of air mass transport through the Tropical Tropopause Layer (TTL) during NH winter

K. Krüger^{1,3}, S. Tegtmeier^{2,3}, and M. Rex³

¹IFM-GEOMAR, Kiel, Germany

²University of Toronto, Toronto, Canada

³Alfred Wegener Institute for Polar and Marine Research, Potsdam, Germany

Received: 11 September 2007 – Accepted: 21 September 2007 – Published: 28 September 2007

Correspondence to: K. Krüger (kkrueger@ifm-geomar.de)

Title Page

Abstract

Introduction

Conclusions

References

Tables

Figures

◀

▶

◀

▶

Back

Close

Full Screen / Esc

Printer-friendly Version

Interactive Discussion

EGU

Abstract

A long-term climatology of air mass transport through the tropical tropopause layer (TTL) is presented, covering the period from 1962–2005. The transport through the TTL is calculated with a Lagrangian approach using radiative heating rates as vertical velocities in an isentropic trajectory model. We demonstrate the improved performance of such an approach compared to previous studies using vertical winds from meteorological analyses. Within the TTL, the averaged diabatic ascent is 0.5 K/day during Northern Hemisphere (NH) winters 1992–2001, close to observations from the tape recorder. Climatological maps show a cooling and strengthening of this part of the residual circulation during the late 1990s and early 2000s compared to the long-term mean. Lagrangian cold point (LCP) fields show systematic differences for varying time periods and natural forcing components. The interannual variability of LCP temperature and density fields are found to be influenced by volcanic eruptions, ENSO, QBO and the solar cycle. The coldest and driest TTL is reached during QBOE and La Niña over the western Pacific, whereas during volcanic eruptions, El Niño and QBOW it is warmer and less dry.

1 Introduction

The tropical tropopause layer (TTL) is the main entrance region for trace gases traveling from the troposphere into the stratosphere. For this reason it is important to understand the underlying dynamical and microphysical processes. Some important factors affecting the trace gas content and variability in the stratosphere are the temperature history of the air parcels, their residence time in the TTL and the geographical distribution of their individual entry points into the stratosphere. A better representation of these factors will also help to clarify which role very short lived substances (VSLs) like bromocarbons could play in depleting stratospheric ozone (WMO, 2007).

Recent investigations show that both horizontal and vertical transport processes in

ACPD

7, 13989–14010, 2007

TTL climatology

K. Krüger et al.

Title Page

Abstract

Introduction

Conclusions

References

Tables

Figures

◀

▶

◀

▶

Back

Close

Full Screen / Esc

Printer-friendly Version

Interactive Discussion

EGU

TTL climatology

K. Krüger et al.

[Title Page](#)[Abstract](#)[Introduction](#)[Conclusions](#)[References](#)[Tables](#)[Figures](#)[◀](#)[▶](#)[◀](#)[▶](#)[Back](#)[Close](#)[Full Screen / Esc](#)[Printer-friendly Version](#)[Interactive Discussion](#)

the TTL play a role in dehydrating air parcels that eventually enter the stratosphere. For this kind of studies trajectory calculations are used (Lagrangian approach), driven by all three wind-components from meteorological assimilations (Bonazzola and Haynes, 2004; Fueglistaler et al., 2004). Fueglistaler and Haynes (2005) were able to show that the observed variability of stratospheric water vapor in the TTL is consistent with the temperature history of air parcels. However, using vertical winds to drive trajectory calculations in the TTL has been shown to result in unrealistic vertical transport while other aspects of transport are well represented (Wohlmann and Rex, 2007¹). But in general, the formulation of vertical transport typically limits our understanding of the dynamical processes in the TTL.

In this study we present a long-term climatology of transport processes in the upper part of the TTL during the cold season (NH winter), covering the operational analyses of the European Centre for Medium Range Weather Forecast (opECMWF) (Simmons et al., 2005) and 40-years of ECMWF reanalysis (ERA40) (Uppala et al., 2005) period. In contrast to previous TTL studies an alternative approach is explored to better constrain the vertical velocities in isentropic trajectory models of this region of the atmosphere: we apply a reverse domain filling trajectory model coupled with a radiative transfer model to calculate diabatic heating rates, that are used as vertical velocities. Such an approach was applied by e.g. Schoeberl et al. (2003).

The following questions will be newly addressed in this study: Does the Lagrangian cold point (LCP) distribution in the TTL derived by this approach differ from previously published results? How fast is the large-scale diabatic ascent in the TTL? How do natural forcing components impact the interannual variability of LCP? The answers will be presented as follows: First the model and method employed are described in Sect. 2. Section 3 highlights the main results for a case study, a climatology and processes influencing the interannual variability. Results are discussed and summarized in Sects. 4 and 5.

¹Wohlmann, I. and Rex, M.: Improvement of vertical and residual velocities in pressure or hybrid coordinates in analysis data in the stratosphere, Geophys. Res. Lett., submitted, 2007.

2 Model and method

For this transport study we are using a trajectory model with a different approach for the TTL. Radiative heating rates (Q) are applied as vertical velocity in a quasi-isentropic trajectory model in the stratosphere to avoid the noisy ((Manney et al., 2005b); Wohltmann and Rex, 2007¹) and too high vertical velocities of meteorological assimilations (Meijer et al., 2004; Scheele et al., 2005; Monge-Sanz et al., 2007). Such an approach can be employed in the stratosphere, where radiative processes are determining the slow mean meridional circulation (Andrews et al., 1987). Calculated diabatic ($Q \neq 0$) heating rates are directly used as vertical velocities in a quasi-isentropic trajectory model ($D\Theta/Dt=Q$, with the potential temperature Θ). For the polar lower and mid-stratosphere (McKenna et al., 2002; Chipperfield, 2006; Tegtmeier et al., 2007²) and for the tropical lower stratosphere (Schoeberl et al., 2003), the usefulness and superiority of this approach was demonstrated. In principle the approach is valid for all levels above the region, where latent heat release (e.g. in convection) contributes significantly to vertical transport. Indeed, even for the upper part of the TTL, the level between the cold point tropopause and the level of net zero heating (WMO, 2007), convincing results were obtained by comparing in-situ observations with our approach (Immler et al., 2007).

The new trajectory model was developed, carefully tested and validated by Tegtmeier et al. (2007)². The trajectories are calculated on isentropic coordinates, using horizontal wind and temperature fields from the ECMWF analyses. As we are interested in the troposphere to stratosphere (TS) transport in the tropics, we perform backward trajectories starting on a stratospheric level to ensure a larger set of tropospheric air masses reaching the stratosphere. The statistical analyses of a large set of trajectories allows us to compare our averaged Lagrangian results with trace gas observations. The net vertical flux of mass is only correctly represented by Lagrangian calculations, that fol-

²Tegtmeier, S., Rex, M., Krüger, K., Wohltmann, I., and Schoellhammer, K.: Variations of the residual circulation in the northern hemispheric winter, J. Geophys. Res., submitted, 2007.

Title Page

Abstract

Introduction

Conclusions

References

Tables

Figures

◀

▶

◀

▶

Back

Close

Full Screen / Esc

Printer-friendly Version

Interactive Discussion

low the air masses and include the interaction between horizontal and vertical motion of air (Tegtmeier et al., 2007²).

Similar as in the study of Bonazzola and Haynes (2004), the backward trajectories are started on a $2^\circ \times 2^\circ$ grid from 30° S to 30° N on the 400 K isentropic level for the period from December to February (DJF). This leads to a total number of $N=5580$ trajectories per winter. The trajectory model is run with a time integration step of 20 min, while the output is stored every 6 h. The heating rates are derived from a stand-alone version of the ECMWF radiative transfer model (Morcrette et al., 1998), using ERA40 and opECMWF temperature, ozone, water vapor, cloud cover and cloud content fields every 6 h. An intercomparison study between the ECMWF and the Fu-Liou radiation scheme was carried out for a case study over Galapagos (Gettelmann et al., 2004), which demonstrated a very good agreement for radiative heating rates within the TTL with differences less than 0.1 K/day (Tegtmeier et al., 2007²).

For both calculations, the meteorological input is interpolated on T106 resolution with a regular $2^\circ \times 2^\circ$ grid. The 60 vertical hybrid coordinate model levels of ERA40 and opECMWF data are used (L60), which results in a vertical resolution of ~ 1 km within the tropical tropopause region. Due to limited data availability this study concentrates on the period 1962/1963 to 2001/2002 for ERA40 and 2000/2001 to 2004/2005 for opECMWF data.

As we are only interested in the TS transport of air masses, the backward trajectories had to pass the isentropic level of 360 K (~ 14 km altitude). For each TS trajectory, the lowest temperature along its path is stored, which corresponds to the location of the LCP. The cold point is almost equal to the minimum saturation mixing ratio tropopause (Zhou et al., 2001). The water vapor saturation mixing ratio over ice e_{ice} at the cold point is calculated after Sonntags formula (Sonntag, 1994) as it was carried out in the companion study by Immler et al. (2007). The Lagrangian diabatic heating (Q_L) is analysed along the trajectory as the average between 400 K and the LCP (\hat{Q}_{LCP}). The climatology and composite maps show averages of the trajectories that experienced their cold point inside a $5^\circ \times 5^\circ$ box. Only grid boxes sampled by trajectories are shown.

TTL climatology

K. Krüger et al.

Title Page

Abstract

Introduction

Conclusions

References

Tables

Figures

◀

▶

◀

▶

Back

Close

Full Screen / Esc

Printer-friendly Version

Interactive Discussion

The density (ν) of the trajectories is given by $\nu=n/(N\cdot ny)$, where N is the total number of all trajectories per winter, n is the number of TS trajectories per winter and ny is the number of years.

3 Results

5 Before the TTL climatology and the interannual variability is presented a case study for the NH winter 2001/2002 is given.

3.1 Case study

Figures 1a–e illustrate the LCPs temperature and the distribution of the LCP which are reached during the three month journey of the trajectories through the TTL. Five different vertical velocity fields were used as input for the trajectory calculations. Four of them are based on heating rates as vertical velocities, calculated with four different ozone fields as input data, and one is based on vertical wind fields to drive vertical transport. Clearly, the opECMWF trajectories (Figs. 1a and b) are among the coldest with LCPs localized over the maritime continent and temperatures well below 180 K, whereas the LCPs in ERA40 have temperatures around 184 K (Figs. 1c and d). A larger geographical spread of the trajectories is found for the cases using climatological ozone fields (Figs. 1b and d), taking the ECMWF standard ozone climatology (Fortuin and Langematz, 1995) as input. These two cases indicate the sensitivity of Q due to different ozone fields in the radiative transfer calculations. Figure 1e using vertical winds of opECMWF is outstanding and leads to the largest geographical dispersion of the trajectories and highest LCP temperatures compared to the other two opECMWF cases. However, the general distribution of the LCPs does not seem to change much between the five cases. For analysing the differences more quantitatively, Fig. 1f displays the density of LCPs over the tropical belt (40° S–40° N) for 5° longitude bins for each of the five input data. The occurrence gives the number of all

Title Page

Abstract

Introduction

Conclusions

References

Tables

Figures

◀

▶

◀

▶

Back

Close

Full Screen / Esc

Printer-friendly Version

Interactive Discussion

trajectory points from Figs. 1a–e, which are hard to distinguish from each other. The cases using heating rates (black, red, green and orange lines) show the maximum occurrence of LCP trajectories over 165° E. For opECMWF with vertical winds (blue line), the maximum occurrence shifts towards 185° E. The highest number of LCP trajectories in the western Pacific region is reached for calculations based on opECMWF and ERA40 data using assimilated ECMWF ozone fields (over 500), whereas the LCPs in calculations based on opECMWF+3D wind show a more zonal distribution and the maximum number over the central Pacific is only 200. This larger geographical dispersion of the trajectories using vertical wind fields is also visible in the smaller total amount of zonal LCP trajectories within 40° S–40° N. For the calculations based on opECMWF heating rates, 58.74% of all LCPs lie in the West Pacific region (as defined by 120° E to 180° E), while for the calculations based on opECMWF vertical winds only 34.32% of the LCPs lie in this region. To better understand the reason for these discrepancies, Fig. 2 presents the probability density function (PDF) of the Lagrangian diabatic velocity for the upper part of the TTL (\hat{Q}_{LCP}). All five lines show their maximum at a positive \hat{Q}_{LCP} as would be expected from the mean upwelling (positive diabatic heating) in the tropical tropopause. ERA40 and opECMWF data (red and black lines) peak at 0.5 K/day and 0.75 K/day heating in contrast to the calculation using the vertical wind from opECMWF (blue line). This PDF shows a broader distribution maximizing at 0.25 K/day for frequencies reaching only 0.18. There is a long tail on both sides of the PDF skewed towards positive heating rates, reaching unrealistically high diabatic velocities of more than 3 K/day, as was also noted by Bonazzola and Haynes (2004). The effect of using the ECMWF standard ozone climatology is illustrated by the green and orange lines, which maximize at 1 and 1.25 K/day with lower frequencies. In the tropical tropopause region there is slightly more ozone in the standard climatology compared to the assimilated fields (not shown here and Oikonomou and O'Neill, 2006), which leads to a stronger heating, hence upwelling in the TTL. The mean diabatic velocity for ERA40 is 0.51 K/day and for opECMWF 0.56 K/day. This value is only 70% of the mean value derived with vertical wind fields of opECMWF (blue line, 0.81 K/day). McFarlane

[Title Page](#)[Abstract](#)[Introduction](#)[Conclusions](#)[References](#)[Tables](#)[Figures](#)[◀](#)[▶](#)[◀](#)[▶](#)[Back](#)[Close](#)[Full Screen / Esc](#)[Printer-friendly Version](#)[Interactive Discussion](#)

et al. (2007) observed heating rates for two tropical stations over the western Pacific for the period March to December 1999 and February to July 2000, which show average heating rates of 0.5 K/day around 17 km altitude, which is in good agreement with our derived heating rates using assimilated ECMWF ozone fields. From an average Q (\hat{Q}) one can directly derive the residence time for a certain altitude range in the TTL given in days per potential temperature layer (altitude difference); a larger \hat{Q} leads to a shorter residence time. From Fig. 2 we derive an averaged residence time of 36/40 days for the 360–380 K layer using opECMWF/ERA40 data with heating rates and only 20 days for the 360–380 K layer using opECMWF with vertical winds. We can directly compare these numbers with the range of published results, which lie in between the large uncertainty range of 20 and 80 days for the 360–380 K layer (WMO, 2007).

Based on comparisons with vertical velocities and vertical diffusion rates derived from trace gas transport Wohltmann and Rex (2007)¹ also show that the mean and the width of the distribution of heating rate calculations are both consistent with observations and much more realistic than the calculations using vertical winds.

Taking the advantage of this improved performance, we are using off-line calculated heating rates as vertical velocity derived from the ECMWF assimilated fields, to analyse the climatology and interannual variability during NH winter.

3.2 Climatology

Figure 3 shows the climatology of LCP temperature, the density of LCPs and the zonal mean \hat{Q}_{LCP} for different time periods. The long-term mean from 1962–2001 displays a large region of LCP temperatures below 188 K over the equator. They are coolest and driest in terms of e_{ice} from the maritime continent towards the central Pacific (below 186 K and 2 ppmv e_{ice}). The highest density of LCP reaches 0.01 just south of this cold point, which leads to the interpretation that less air masses are sampled directly through the coldest region. Comparing with Fueglistaler et al. (2005), who show a climatology map for the period 1979–2001, the location of the highest density of air masses crossing the LCP is very similar to our calculations. But as noted above, the

Title Page

Abstract

Introduction

Conclusions

References

Tables

Figures

◀

▶

◀

▶

Back

Close

Full Screen / Esc

Printer-friendly Version

Interactive Discussion

TTL climatology

K. Krüger et al.

[Title Page](#)[Abstract](#)[Introduction](#)[Conclusions](#)[References](#)[Tables](#)[Figures](#)[◀](#)[▶](#)[◀](#)[▶](#)[Back](#)[Close](#)[Full Screen / Esc](#)[Printer-friendly Version](#)[Interactive Discussion](#)

LCPs in our calculations are even more focussed in this region and overall the distribution is less zonal. Two secondary maxima are located over central America and over the African equator. The middle panel presents the shorter period 1992–2001, where satellite measurements for stratospheric water vapor are available. During this period the LCPs are colder and drier compared to the long-term mean. The minimum in LCP temperature is located over Micronesia, whereas the region with the highest density of LCPs lies just southeast of it. In the lower panel, the opECMWF period is shown to contrast the extremely cold and dry TTL winters from 2000–2004. The LCP temperatures indicate values below 184 K (~ 1.25 ppmv e_{ice}) over the maritime continent and western Pacific accompanied with a westward shift of the LCP density compared to the period 1992–2001. Bearing in mind that opECMWF zonal mean temperatures seem to have a cold bias compared to ERA40 data of -1 K in average at 100 hPa (Dhomse et al., 2006), this analysed change of -2 K to -4 K in LCP has to be interpreted accordingly. This will be discussed in more detail in Sect. 4.

Corresponding with the enhanced wave driving in the NH, observed since the late 1990s and early 2000s (Randel et al., 2006), an increase of diabatic ascent is analysed for the 2000–2004 period compared to the long-term climatology. The weaker diabatic ascent during 1992–2001 in ERA40 data agrees with the weaker wave driving during the cold polar NH winters in the 1990s, but disagrees with the lower LCP temperatures found over the western Pacific during 1992–2001 compared to 1962–2001. Inspecting maps of \hat{Q}_{LCP} (not shown here) reveal local maxima over the western Pacific of 0.6 K/day during 1962–2001, 0.7 K/day during 1992–2001 and up to 0.8 K/day during 2000–2004. For all three periods maximum zonal mean \hat{Q}_{LCP} is reached north of the equator, indicating the influence of enhanced planetary wave activity of the winter hemisphere. According to the model study by Haynes et al. (1991) an influence of extratropical wave driving is found only on the winterward side of the tropics during periods of transient fluctuations (e.g. the occurrence of major midwinter warmings (MW)). During the period 1998/1999 and 2003/2004 seven MW were observed during these six winters in the NH, which is unprecedented in the record (Manney et al., 2005a). In

the Southern Hemisphere the first recorded MW took place in September 2002 (Krüger et al., 2005) accompanied by a general increase of wave driving since 2000 (Dhomse et al., 2006). Corresponding to this, we find an enhanced diabatic ascend of 0.6 K/day in the Southern Hemisphere tropics during 2000–2004 in contrast to only 0.5 K/day in earlier time periods.

3.3 Interannual variability

In this section natural forcing components are investigated in more detail, which are known to have an influence on the tropical tropopause region. Matching years of data are sorted into categories according to volcanic eruptions, El Niño Southern Oscillation (ENSO), the Quasi-Biennial Oscillation (QBO) and the solar cycle (e.g. Labitzke et al., 2006, and related work), using the ERA40 time series. The influence of volcanoes, ENSO and QBO on the TTL was already investigated by several authors (e.g. Randel et al., 2000; Zhou et al., 2001; Gettelmann et al., 2001; Bonazzola and Haynes, 2004; Zhou et al., 2004; Fueglistaler and Haynes, 2005) taking an Eulerian framework or concentrating on shorter time periods using vertical wind fields. Figure 4 illustrates composite maps and anomalies of LCP temperatures and density for different processes. The coldest and driest TTL in average is reached during the QBO Easterly phase (QBOE) and La Niña years north of the maritime continent with LCP temperatures below 184 K (~ 2 ppmv). The QBOE composites display a zonally uniform cold anomaly along the tropical belt from 20° S to 20° N of -1 to -2 K (-0.5 ppmv) compared to the long-term mean. This is in contrast to La Niña composites, which display a longitudinal shift of colder air over the Indian Ocean and western Pacific region and warmer air over the central/eastern Pacific. The maximum density of LCPs lies over the central Pacific for QBOE and is shifted westward towards the maritime continent for La Niña years, as would be expected from the location of the main convection zones observed during La Niña. The highest LCP temperatures (186 K) are reached during volcanic eruptions and El Niño having an opposite pattern compared to La Niña composites. A positive warm pool (exceeding 4 K) is found over the eastern Pacific for La Niña, which

Title Page

Abstract

Introduction

Conclusions

References

Tables

Figures

◀

▶

◀

▶

Back

Close

Full Screen / Esc

Printer-friendly Version

Interactive Discussion

is not visible in such a strength in Eulerian based studies (Gettelmann et al., 2001; Zhou et al., 2001) and might be due to the small sample of trajectories in this region (15 to 60 trajectories per grid box). In contrast to La Niña, the LCP density for El Niño is maximizing over the central/eastern Pacific in good correspondence with the shift of the convection center during El Niño. The QBO Westerly (QBOW) phase displays a zonally symmetric warmer LCP up to 1 K.

The physical mechanisms of the solar cycle influence on the atmosphere are discussed in the study by e.g. Kodera and Kuroda (2002). Taking solar maximum and minimum (SMAX and SMIN) into account, a zonally asymmetric structure appears with colder LCP over the Indian Ocean and western Pacific (-1 K) and a warmer LCP over the central/eastern Pacific (2 to 3 K) for SMAX. The opposite signal exists for SMIN with smaller temperature difference asymmetries than for SMAX. Areas of lower LCP temperatures correspond to an increased number of trajectory crossing the cold point, shifted towards the western/eastern Pacific for SMAX/SMIN years. The reason for this asymmetric response of the solar cycle on the TTL seems to be related with a westward shift of the Walker circulation during SMAX (van Loon et al., 2007). Zonally averaging the composites leads to a systematic higher LCP temperature of 0.2 K during SMAX compared to SMIN (not shown here), which is in good agreement with the study by e.g. Labitzke et al. (2006).

4 Discussion

The results might be affected by the inhomogeneities of the ERA40 time series (Uppala et al., 2005) and between ERA40 and opECMWF analyses. The observed cooling in the tropical tropopause region has been investigated by many authors (e.g. Fueglistaler and Haynes, 2005; Randel et al., 2006). It exists in different available meteorological data sets since the mid 1990s as was investigated by Dhomse et al. (2006), who also found a cold bias in opECMWF compared to ERA40 data of -1 K at the 100 hPa level during 2001/2002. However, comparing the cold point temperature between ra-

Title Page

Abstract

Introduction

Conclusions

References

Tables

Figures

◀

▶

◀

▶

Back

Close

Full Screen / Esc

Printer-friendly Version

Interactive Discussion

diosonde measurements, opECMWF (L60) and ERA40 (L60) analyses for five tropical stations revealed a good agreement between opECMWF and radiosondes, whereas ERA40 analysis has a warm bias around 2 K (Brunn and Krüger, SCOUT-O3 annual meeting in Crete 2007). These results are in contrast to the above mentioned references, which concentrated on temperature differences at standard pressure levels. Assuming that opECMWF data do not have or at most a slight cold bias of -1 K in LCP, a cooling (we analyse a peak of -4 K, Fig. 3) and enhanced upwelling during the late 1990s (ERA40) and early 2000s (opECMWF) would still exist. The case study for NH winter 2001/2002 displays a shift towards higher \hat{Q}_{LCP} for opECMWF data compared to ERA40, which is in agreement with the cold bias between them. \hat{Q} derived from the “tape recorder” shows a zonally averaged heating of ~ 0.4 K/day in the TTL during NH winter (Mote et al., 1996), which is in good correspondence to our tropical average \hat{Q}_{LCP} of 0.5 K/day for the period 1992–2001.

Comparing our Lagrangian diabatic ascend rates with studies using the conventional method we find large differences. Using vertical winds of ERA40 (Fueglistaler et al., 2004) and opECMWF analyses (Levine et al., 2007, and this study) for the NH winter 2000/2001, a residence time of 20 days for the 360–380 K layer is derived. Whereas using our new approach with diabatic heating rates we find an average of 38 days (ERA40) and 48 days (opECMWF) for the 360–380 K layer during 2000/2001 (not shown) and 40/36 days for ERA40/opECMWF during 2001/2002. The differences between the two ECMWF analyses indicate the above mentioned inhomogeneities of the ECMWF assimilations. Our results lie in the middle of the uncertainty range of 20 and 80 days for the 360–380 K layer published by WMO (2007), which are only given for single years. To study the interannual variability of the residence time is important for long-term transport studies of VLSLs and to limit the range of uncertainty within the TTL, which will be investigated in more detail in a future study.

The geographical distribution of the LCP is very robust and does not seem to be much affected by using our method compared to the vertical wind method (this study, Bonazzola and Haynes, 2004; Fueglistaler et al., 2005). However, differences in the

Title Page

Abstract

Introduction

Conclusions

References

Tables

Figures

◀

▶

◀

▶

Back

Close

Full Screen / Esc

Printer-friendly Version

Interactive Discussion

density of trajectories, distribution of \hat{Q}_{LCP} and in residence time are large. These are important for troposphere-stratosphere transport processes and particularly for the chemistry of VSLS in the TTL and need to be further investigated.

5 Conclusions

5 Multi-year calculations of radiative heating rates and isentropic trajectories have been carried out to investigate air mass transport through the TTL with a new approach. Investigating the influence of different vertical velocities for one NH winter 2001/2002 demonstrates the great advantage of using diabatic heating rates to overcome known problems with vertical winds of meteorological assimilation systems. In correspon-

10 dence to the NH winter 2001/2002, a mean residence time of ~ 40 days for the 360–380 K layer is also found for the NH winter 2000/2001. This time is twice as long as derived from trajectory calculations using vertical winds from ECMWF assimilations (Fueglistaler et al., 2004; Levine et al., 2007, and this study). A companion study by Immler et al. (2007) demonstrated that cirrus occurrence, which is simulated using our

15 trajectories with diabatic heating rates, are well correlated with lidar observations of tropical cirrus. In contrast, these authors found no such correlation when using trajectories based on vertical winds. Applying more realistic vertical velocities does have a large impact on transport studies in the TTL, in particular on transport of VSLS released from the surface.

20 Long-term calculations of transport processes in the TTL during NH winter show the following new results:

1. The coldest and driest TTL is predicted north of the maritime continent during the late 1990s and early 2000s together with an increase of zonally averaged diabatic ascent. This increase of upwelling is consistent with an enhanced stratospheric wave driving observed since the late 1990s (Randel et al., 2006; Dhomse et al., 2006).

Title Page

Abstract

Introduction

Conclusions

References

Tables

Figures

◀

▶

◀

▶

Back

Close

Full Screen / Esc

Printer-friendly Version

Interactive Discussion

TTL climatology

K. Krüger et al.

2. We examine the influence of several natural processes affecting the interannual variability in the TTL. Volcanic eruptions, ENSO events and the QBO phases show an impact on the pattern and magnitude of Lagrangian cold point temperatures and density of trajectories. The coldest and driest TTL is reached during QBOE and La Niña north of the maritime continent, whereas during volcanic eruptions, El Niño and QBOW a warmer and less dry TTL is detected.

3. Unique for TTL transport studies, the solar cycle effect is analysed with an Lagrangian approach. During SMAX years we found a colder TTL (higher density of trajectories) over the Indian Ocean/western Pacific and during SMIN years a colder TTL over the eastern Pacific/Atlantic.

ENSO, volcanoes and solar cycle composites exhibit a longitudinal asymmetry, whereas the QBO presents a zonally symmetric structure in the TTL. In contrast to Zhou et al. (2001) larger differences in LCP fields are found for ENSO and QBO phases, demonstrating the advantage of using a Lagrangian approach, which takes the air masses sampling into account. The overlapping influence of ENSO, QBO and solar cycle phases on transport processes in the TTL should be taken into account, which is beyond the scope of this paper and will be investigated in a future study.

Acknowledgements. We would like to thank J.-J. Morcrette for providing the ECMWF radiation code. The meteorological analyses were supplied by ECMWF. The authors thank I. Wohltmann and three anonymous reviewers for their useful comments, which helped to improve this paper. This study was supported by the European Union's 6th framework program within the SCOUT-O₃ (GOCE-CT-2004-505390) project.

References

Andrews, D. G., Holton, J. R., and Leovy, C. B.: Middle atmosphere dynamics, Academic Press, 1987. [13992](#)

[Title Page](#)[Abstract](#)[Introduction](#)[Conclusions](#)[References](#)[Tables](#)[Figures](#)[I◀](#)[▶I](#)[◀](#)[▶](#)[Back](#)[Close](#)[Full Screen / Esc](#)[Printer-friendly Version](#)[Interactive Discussion](#)

- Bonazzola, M. and Haynes, P.: A trajectory-based study of the tropical tropopause region, *J. Geophys. Res.*, 109, D20112, doi:10.1029/2003JD004356, 2004. [13991](#), [13993](#), [13995](#), [13998](#), [14000](#)
- Chipperfield, M.: New version of the TOMCAT/SLIMCAT off-line chemical transport model: Intercomparison of stratospheric tracer experiments, *Q. J. Roy. Meteorol. Soc.*, 132, 2006, doi:10.1256/qj.05.51, 2006. [13992](#)
- Dhomse, S., Weber, M., and Burrows, J.: The relationship between tropospheric wave forcing and tropical lower stratospheric water vapor, *Atmos. Chem. Phys. Discuss.*, 6, 9563–9581, 2006, <http://www.atmos-chem-phys-discuss.net/6/9563/2006/>. [13997](#), [13998](#), [13999](#), [14001](#)
- Fortuin, J. P. F. and Langematz, U.: An update on the global ozone climatology and on concurrent ozone and temperature trends, *Proc. SPIE, Atmos. Sensing and Modeling*, 2311, 207–216, 1995. [13994](#)
- Fueglistaler, S., Wernli, H., and Peter, T.: Stratospheric water vapor predicted from the Lagrangian temperature history of air entering the stratosphere in the tropics, *J. Geophys. Res.*, 110, D03108, doi:10.1029/2003JD004069, 2004. [13991](#), [14000](#), [14001](#)
- Fueglistaler, S. and Haynes, P.: Control of interannual and longer-term variability of stratospheric water vapor, *J. Geophys. Res.*, 110, D24108, doi:10.1029/2005JD006019, 2005. [13991](#), [13998](#), [13999](#)
- Fueglistaler, S., Bonazzola, M., Haynes, P. H., and Peter, T.: Stratospheric water vapor predicted from the Lagrangian temperature history of air entering the stratosphere in the tropics, *J. Geophys. Res.*, 110, D08107, doi:10.1029/2004JD005516, 2005. [13996](#), [14000](#)
- Gettelman, A., Randel, W., Massie, S., Wu, F., Read, W., and Russell III, J.: El Niño as a natural experiment for studying the tropical tropopause region, *J. Climate*, 14, 3375–3391, 2001. [13998](#), [13999](#)
- Gettelman, A., de Forster, P., Fujiwara, M., Fu, Q., Vömel, H., Gohar, L., Johanson, C., and Ammerman, M.: Radiation balance of the tropical tropopause layer, *J. Geophys. Res.*, 109, doi:10.1029/2003JD004190, 2004. [13993](#)
- Haynes, P., Marks, C., McIntyre, M., Shepherd, T., and Shine, K.: On the “Downward Control” of extratropical diabatic circulations by eddy-induced zonal mean forces, *J. Atmos. Sci.*, 49, 651–679, 1991. [13997](#)
- Immler, F., Krüger, K., Tegtmeier, S., Fujiwara, M., Fortuin, P., Verver, Gé., and Schrems, O.: Cirrus clouds, humidity, and dehydration in the tropical tropopause layer observed

[Title Page](#)[Abstract](#)[Introduction](#)[Conclusions](#)[References](#)[Tables](#)[Figures](#)[◀](#)[▶](#)[◀](#)[▶](#)[Back](#)[Close](#)[Full Screen / Esc](#)[Printer-friendly Version](#)[Interactive Discussion](#)

- at Paramaribo, Suriname (5.8° N, 55.2° W), *J. Geophys. Res.*, 112, D03209, doi:10.1029/2006JD007440, 2007. [13992](#), [13993](#), [14001](#)
- Kodera, K. und Kuroda, Y.: Dynamical response to the solar cycle, *J. Geophys. Res.*, 107, 4749, doi:10.1029/2002JD002224, 2002. [13999](#)
- 5 Krüger, K., Naujokat, B., and Labitzke, K.: The unusual midwinter warming in the southern hemisphere stratosphere 2002: a comparison to northern hemisphere phenomena, *J. Atmos. Soc.*, 62, 603–613, 2005. [13998](#)
- Labitzke, K., Kunze, M., and Brönnimann, S.: Sunspots, the QBO, and the Stratosphere in the North Polar Region – 20 Years later, *Met. Zeit.*, 15(3), 355–363, 2006. [13998](#), [13999](#)
- 10 Levine, J., Braesicke, P., Harris, N., Savage, N., and Pyle, J.: Pathways and timescales for troposphere-to-stratosphere transport via the tropical tropopause layer and their relevance for very short lived substances, *J. Geophys. Res.*, 112, D04308, doi:10.1029/2005JD006940, 2007. [14000](#), [14001](#)
- Manney, G., Krüger, K., Sabutis, J., Sena, S., and Pawson, S.: The remarkable 2003-2004 winter and other recent warm winters in the Arctic stratosphere since the late 1990s, *J. Geophys. Res.*, 110, D04107, doi:10.1029/2004JD005367, 2005a. [13997](#)
- 15 Manney, G., Allen, D., Krüger, K., Sabutis, J., Pawson, S., Swinbank, R., Randall, C., Simmons, A., and Long, C.: Diagnostic comparison of meteorological analyses during the 2002 Antarctic winter, *Mon. Weather Rev.*, 133, 1261–1278, 2005b. [13992](#)
- 20 McFarlane, S., Mather, J., and Ackerman, T.: Analysis of tropical radiative heating profiles: A comparison of models and observations, *J. Geophys. Res.*, 112, D14218, doi:10.1029/2006JD008290, 2007. [13995](#)
- McKenna D. S., Konopka, P., Groöf, J.-U., Günther, G., Müller, R., Spang, R., Offerman, D., and Orsolini, Y.: A new Chemical Lagrangian Model of the Stratosphere (ClAMS), 1, Formulation of advection and mixing, *J. Geophys. Res.*, 107(D16), 4332, doi:10.1029/2000JD000114, 2002. [13992](#)
- 25 Meijer, E. W., Bregman, B., Segers, A., and van Velthoven, P. F. J.: The influence of data assimilation on the age of air calculated with a global chemistry-transport model using ECMWF wind fields, *Geophys. Res. Lett.*, 31(23), L23114, doi:10.1029/2004GL021158, 2004. [13992](#)
- 30 Monge-Sanz, B., Chipperfield, M., Simmons, A., and Uppala, S.: Mean age of air and transport in a CTM: comparison of different ECMWF analyses, *Geophys. Res. Lett.*, 34, L04801, doi: 10.1029/2006GL028515, 2007. [13992](#)
- Mote, P., Rosenlof, K., McIntyre, M., Carr, E., Gille, J., Holton, J., Kinnnersley, J., Pumphrey,

TTL climatology

K. Krüger et al.

Title Page

Abstract

Introduction

Conclusions

References

Tables

Figures

◀

▶

◀

▶

Back

Close

Full Screen / Esc

Printer-friendly Version

Interactive Discussion

TTL climatology

K. Krüger et al.

Title Page

Abstract

Introduction

Conclusions

References

Tables

Figures

◀

▶

◀

▶

Back

Close

Full Screen / Esc

Printer-friendly Version

Interactive Discussion

H., Russell III, J., and Waters, J.: An atmospheric tape recorder: The imprint of tropical tropopause temperatures on stratospheric water vapor, *J. Geophys. Res.*, 101(D2), 3989–4006, doi:0.029/95JD03422, 1996. [14000](#)

Morcrette, J.-J., Clough, S., Mlawer, E., and Iacono, M.: Impact of a validated radiative transfer scheme, RRTM, on the ECMWF model climate and 10-day forecasts, ECMWF Technical Memo No. 252, pp 47, 1998. [13993](#)

Oikonomou, E. and O'Neill, A.: Evaluation of ozone and water vapor fields from the ECMWF reanalysis ERA40 during 1991-1999 in comparison with UARS satellite and MOZAIC aircraft observations, *J. Geophys. Res.*, 111, D14109, doi:10.1029/2004JD005341, 2006. [13995](#)

Randel, W., Wu, F., and Gaffen, D.: Interannual variability of the tropical tropopause derived from radiosonde data and NCEP reanalysis, *J. Geophys. Res.*, 105, 15 509–15 524, 2000. [13998](#)

Randel, W., Wu, F., Nedoluha, G., Vömel, H., and Forster, P.: Decreases in stratospheric water vapor since 2001: Links to changes in the tropical tropopause and the Brewer-Dobson circulation, *J. Geophys. Res.*, 111, D12312, doi:10.1029/2005JD006744, 2006. [13997](#), [13999](#), [14001](#)

Scheele, M., Siegmund, P., and van Velthoven, P.: Stratospheric age of air computed with trajectories based on various 3D-Var and 4D-Var data sets, *Atmos. Chem. Phys.*, 5, 1–7, 2005, <http://www.atmos-chem-phys.net/5/1/2005/>. [13992](#)

Schoeberl, M., Douglass, A., Zhu, Z., and Pawson, S.: A comparison of the lower stratospheric age spectra derived from a general circulation model and two data assimilation systems, *J. Geophys. Res.*, 108, 4113, doi:10.1029/2002JD002652, 2003. [13991](#), [13992](#)

Simmons, A., Hortal, M., Kelly, G., McNally, A., Untch, A., and Uppala, S.: ECMWF Analyses and Forecasts of Stratospheric Winter Polar Vortex Breakup: September 2002 in the Southern Hemisphere and Related Events, *J. Atmos. Sci.*, 62(3), 668–689, 2005. [13991](#)

Sonntag, D.: Advances in the field of hygrometry, *Meteorologische Zeitschrift*, 3, 51–66, 1994. [13993](#)

Uppala, S. M., Kållberg, P. W., Simmons, A. J., Andrae, U., Da Costa, V., Bechtold, Fiorino, M., Gibson, J. K., Haseler, J., Hernandez, A., Kelly, G. A., Li, X., Onogi, K., Saarinen, S., Sokka, N., Allan, R. P., Andersson, E., Arpe, K., Balmaseda, M. A., Beljaars, A. C. M., Van De Berg, L., Bidlot, J., Bormann, N., Caires, S., Chevallier, F., Dethof, A., Dragosavac, M., Fisher, M., Fuentes, M., Hagemann, S., Hólm, E., Hoskins, B. J., Isaksen, L., Janssen, P. A.

E. M., Jenne, R., McNally, A. P., Mahfouf, J.-F., Morcrette, J.-J., Rayner, N. A., Saunders, R. W., Simon, P., Sterl, A., Trenberth, K. E., Untch, A., Vasiljevic, D., Viterbo, P., and Woollen, J.: The ERA-40 re-analysis, Q. J. Roy. Meteor. Soc., 131, 2961-3012, doi:10.1256/qj.04.176 2005. [13991](#), [13999](#)

5 van Loon, H., Meehl, G., and Shea, D.: Coupled air-sea response to solar forcing in the Pacific region during northern winter, J. Geophys. Res., 112, D02108, doi:10.1029/2006JD007378, 2007. [13999](#)

World Meteorological Organization: Scientific Assessment of Ozone Depletion: 2006, WMO Global Ozone Research and Monitoring Project, Report No. 50, 2007. [13990](#), [13992](#), [13996](#),
10 [14000](#)

Zhou, X., Geller, M., and Zhang, M.: Tropical cold point tropopause characteristics from ECMWF reanalyses and soundings, J. Climate, 14, 1823–1838, 2001. [13993](#), [13998](#), [13999](#),
[14002](#)

15 Zhou, X., Geller, M., and Zhang, M.: Temperature fields in the tropical tropopause transition layer, J. Climate, 17, 2901–2908, 2004. [13998](#)

ACPD

7, 13989–14010, 2007

TTL climatology

K. Krüger et al.

Title Page

Abstract

Introduction

Conclusions

References

Tables

Figures

◀

▶

◀

▶

Back

Close

Full Screen / Esc

Printer-friendly Version

Interactive Discussion

EGU

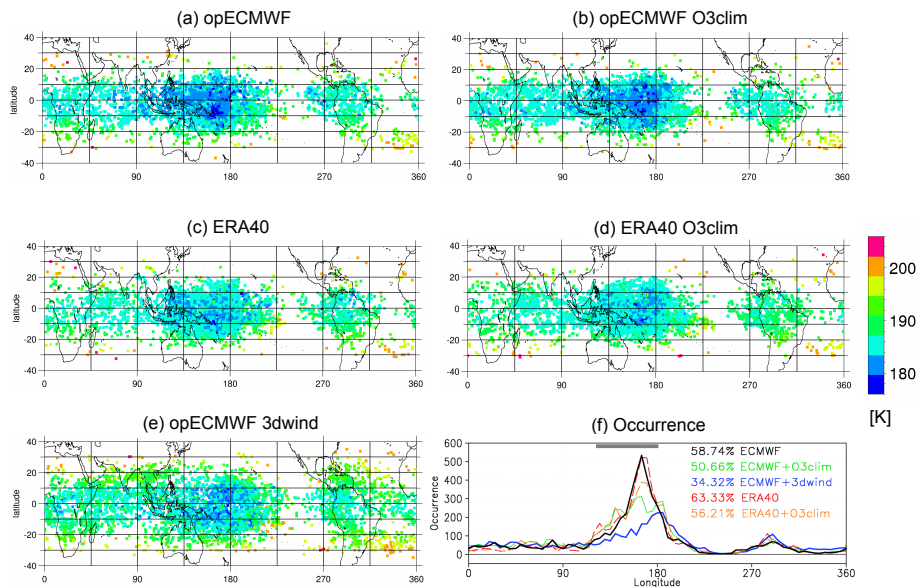


Fig. 1. Maps of LCP temperature [K] during DJF 2001/2002 for **(a)** opECMWF heating rates (black line in f), **(b)** opECMWF heating rates derived from climatological ozone (green line in f), **(c)** ERA40 heating rates (red line in f), **(d)** ERA40 heating rates derived from climatological ozone (orange line in f), **(e)** opECMWF vertical wind (blue line in f). Each square marks one trajectory. **(f)** Occurrence of LCP trajectories averaged over 40° S–40° N, inside 5° longitude bins. The numbers in % indicate the percent of trajectories traveling through the 120° E–180° E region.

[Title Page](#)
[Abstract](#)
[Introduction](#)
[Conclusions](#)
[References](#)
[Tables](#)
[Figures](#)
[◀](#)
[▶](#)
[◀](#)
[▶](#)
[Back](#)
[Close](#)
[Full Screen / Esc](#)
[Printer-friendly Version](#)
[Interactive Discussion](#)

TTL climatology

K. Krüger et al.

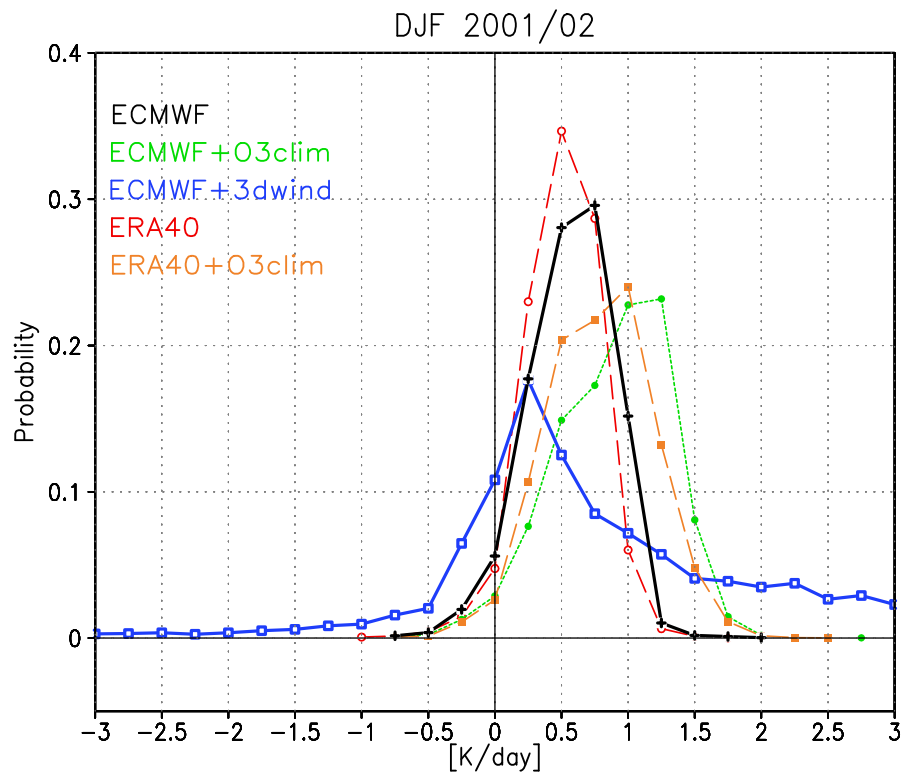


Fig. 2. Probability of \hat{Q}_{LCP} (K/day) for DJF trajectories 2001/02, taking 0.25 K/day bins into account. The color code is as in Fig. 1f.

[Title Page](#)[Abstract](#)[Introduction](#)[Conclusions](#)[References](#)[Tables](#)[Figures](#)[◀](#)[▶](#)[◀](#)[▶](#)[Back](#)[Close](#)[Full Screen / Esc](#)[Printer-friendly Version](#)[Interactive Discussion](#)

EGU

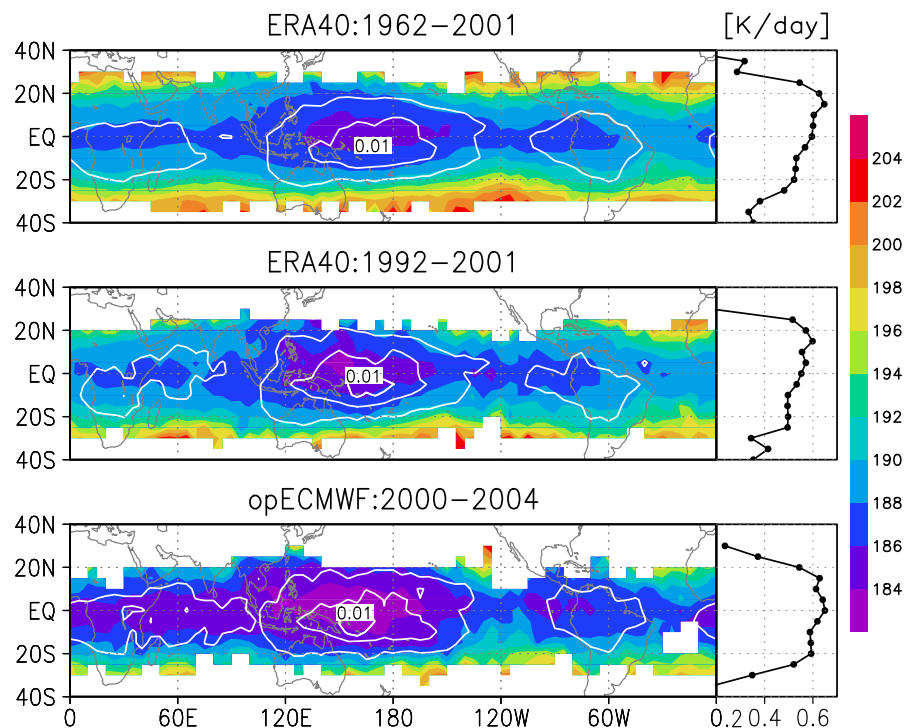


Fig. 3. DJF long-term climatology; Left: LCP temperature [K] (color) and the density of LCPs (white contours); Right: Zonal mean \bar{Q}_{LCP} [K/day]. Top panel: 1962/1963–2001/2002 ERA40 data; middle panel: 1992/1993–2001/2002 ERA40 data; lower panel: opECMWF data from 2000/2001–2004/2005. Contour intervals for the density are 0.001, 0.005 and 0.01 per $5^\circ \times 5^\circ$ grid.

[Title Page](#)
[Abstract](#)
[Introduction](#)
[Conclusions](#)
[References](#)
[Tables](#)
[Figures](#)
[◀](#)
[▶](#)
[◀](#)
[▶](#)
[Back](#)
[Close](#)
[Full Screen / Esc](#)
[Printer-friendly Version](#)
[Interactive Discussion](#)

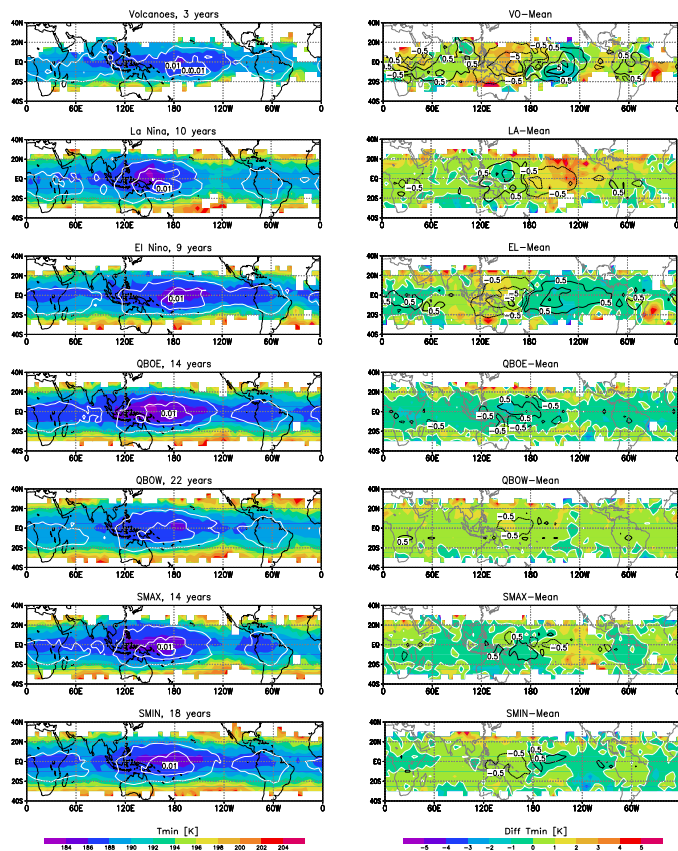


Fig. 4. Left side: DJF composite maps of LCP temperature [K] and density, using the ERA40 time series. Included are: volcanic eruptions, La Niña, El Niño, QBOE, QBOW, SMAX and SMIN; number of years are indicated in the title. Right side: DJF anomalies of composite maps from the 1962–2001 period (Fig. 3) of LCP temperature [K] and density. Intervals for the density differences are 0.5, 2.5 and 5×1000^{-1} per $5^\circ \times 5^\circ$ grid.

[Title Page](#)
[Abstract](#)
[Introduction](#)
[Conclusions](#)
[References](#)
[Tables](#)
[Figures](#)
[Back](#)
[Close](#)
[Full Screen / Esc](#)
[Printer-friendly Version](#)
[Interactive Discussion](#)